

Complexity via Replica Trick

Mohsen Alishahiha,^a Souvik Banerjee,^{b,c} Joshua Kames-King^d

^a*School of Physics, Institute for Research in Fundamental Sciences (IPM),
P.O. Box 19395-5531, Tehran, Iran*

^b*Institut für Theoretische Physik und Astrophysik, Julius-Maximilians-Universität Würzburg,
Am Hubland, 97074 Würzburg, Germany*

^c*Würzburg-Dresden Cluster of Excellence ct.qmat*

^d*Bethe Center for Theoretical Physics and Physikalisches Institut der Universität Bonn, Nussallee
12, 53115 Bonn, Germany*

E-mail: alishah@ipm.ir, souvik.banerjee@physik.uni-wuerzburg.de,
jvakk@yahoo.com

ABSTRACT: We consider the complexity of a single-sided AdS black hole as modelled by an end-of-the-world brane. In addition we present multi-boundary partition functions and matter correlation functions for such a setting. We compute the complexity using a modified replica trick corresponding to the “quenched geodesic length” in JT gravity. The late time behaviour of complexity shows a saturation to a constant value of order e^{S_0} following a period of linear growth. Furthermore, we show that our approach leads to an improved result for the variance of complexity, namely it being time-independent at late times. We conclude by commenting on the introduction of dynamical end-of-the-world branes.

Contents

1	Introduction	1
2	Lorentzian JT gravity with EOW Branes and Wavefunctions	4
2.1	The classical solution	4
2.2	Quantisation in presence of a brane	4
2.3	The disk wavefunctions	7
2.4	The trumpet wavefunctions	8
2.5	Pure vs. Thermal States	10
3	Partition Function	12
4	Correlation Functions	13
5	The late time behaviour of complexity	15
5.1	The geodesic ℓ	16
5.2	The geodesic L	17
5.3	The variance of complexity	21
6	Conclusion and Outlook	22

1 Introduction

In the context of the AdS/CFT correspondence [1–3] it is believed that the interior of a black hole may be systematically studied via the notion of quantum computational complexity. This field of study quantifies the difficulty of constructing a specific “target state” by use of a simple set of “universal gates”. More specifically in a holographic setting it is conjectured that for a chaotic CFT the growth of complexity has a simple geometric description in terms of the growth of the black hole interior.

One of the arguments for this conjecture is that for a fast-scrambling system with finite entropy S , complexity is expected to grow for exponentially large times in the entropy, long after thermal equilibrium has been reached [4, 5]. Remarkably, the same growth holds for the black hole interior. Therefore a concrete instantiation of this conjectured duality is the “complexity=volume” (CV) conjecture, which proposes that the complexity equals the volume of a maximal slice in the black hole interior [4, 6]. There is also another competing proposal known as the “complexity=action” (CA) conjecture, in which the on-shell action on a Wheeler-de Witt patch is determined [7, 8].

We note however, that for chaotic Hamiltonians (as can, for example, be seen in simple circuit models) after the aforementioned period of growth, at times $t \sim (\mathcal{O}(e^S))$ we expect saturation to a plateau of size $C \sim (\mathcal{O}(e^S))$ [9–14]. While semi-classical contributions both in form of the CV and CA conjectures indeed furnish the period of growth, the saturation to the plateau, until recently, has been illusive.

To understand complexity better one may study this concept in Jackiw-Teitelboim (JT) gravity; a theory of two-dimensional dilaton gravity, including arbitrary genus, hyperbolic Riemann surfaces and therefore also exponentially small corrections to semi-classical gravity calculations [15–20]. Actually extending the gravitational sector by including such geometries with an arbitrary number of asymptotic boundaries and arbitrary genus corrects the partition function to be equivalent to a specific double-scaled Hermitian matrix integral. This implies that JT gravity follows RMT universality at late times and therefore exhibits spectral statistics with a dip-ramp-plateau structure [19–22].¹ By use of the same theory it has also been shown that the inclusion of higher topologies gives a unitary Page curve [25, 26].

Recently, holographic complexity was calculated in JT gravity using the CV conjecture in [27] where it was shown that including higher genus geometries (as mentioned above) gives the correct late-time behaviour for complexity. More precisely, in this paper the authors compute complexity in terms of a non-perturbative geodesic length in JT gravity as follows

$$\langle \ell \rangle = \lim_{\Delta \rightarrow 0} \left\langle \sum_{\gamma} \ell_{\gamma} e^{-\Delta \ell_{\gamma}} \right\rangle_{\text{JT}}, \quad (1.1)$$

where γ refers to non self-intersecting geodesics, Δ is a regulator and $\langle \rangle_{\text{JT}}$ a correlator in JT gravity defined over arbitrary genus. It is then argued that in practice (1.1) is calculated by

$$\langle \ell(t) \rangle = - \lim_{\Delta \rightarrow 0} \frac{\partial \langle \chi(t) \chi(0) \rangle_{\text{non-int.}}}{\partial \Delta}, \quad (1.2)$$

where $\langle \chi(t) \chi(0) \rangle_{\text{non-int.}}$ is obtained in the Euclidean JT theory and then analytically continued. Here Δ is the scaling dimension of the operator χ . Eq. (1.2) then of course involves (on surfaces with $g \geq 1$) an infinite number of geodesics which can be taken care of by the moduli space volume of hyperbolic surfaces [28]. It was, then, demonstrated that the above definition results in the following expression for complexity

$$\langle \ell(t) \rangle = - \frac{2e^{-S_0}}{Z(\beta)} \int_0^{\infty} \frac{\langle \rho(s_1) \rho(s_2) \rangle}{\bar{s} \sinh(2\pi \bar{s}) \omega \sinh(\pi \omega)} \exp \left(-\beta \left(\frac{\bar{s}^2}{2} + \frac{\omega^2}{8} \right) - i\bar{s}\omega t \right). \quad (1.3)$$

with the definitions of $\omega = s_1 - s_2$, $\bar{s} = \frac{s_1 + s_2}{2}$ and $s_{1,2} = \sqrt{E_{1,2}}$. The quantity (1.3) was called “spectral complexity” in [27], which can be calculated for any quantum theory by use of its spectral correlation $\langle \rho(s_1) \rho(s_2) \rangle$.

Due to the usual arguments regarding quantum chaos [29, 30], one would suspect that for chaotic systems, (1.3) would reduce to RMT predictions at late times. For the case of JT gravity, the spectral two-point function can be shown to take on the standard RMT sine-kernel structure [20, 22, 31] by use of doubly non-perturbative effects. This in turn leads to the aforementioned, expected behaviour for the quantity $\langle \ell(t) \rangle$: early linear growth followed by a late-time plateau saturation.

In the present work, we are interested in studying two aspects of complexity for JT gravity. First, we would like to use an approach which removes the worrisome behaviour of the variance obtained in [27], as we will explain in greater detail below. Secondly, we would like to study the introduction of an end-of-the-world (EOW) brane. Recently, these

¹For work on the relationship between chaos universality and Euclidean wormholes in higher dimensions see [23, 24].

objects have played a crucial role in understanding quantum aspects of black holes in a two-dimensional setting as they can be used to model black hole microstates in JT gravity [26]. Since a black hole with an EOW brane behind the horizon may be understood as a \mathbb{Z}_2 quotient of the two-sided scenario, it corresponds to a pure state [32, 33]. However, according to the eigenstate thermalisation hypothesis (ETH) [29, 30], a pure state is in many ways indistinguishable from a thermal state.

It is also worth mentioning that EOW branes may also be used in a dynamical manner, which means they appear as loops and are summed over in the path integral. In this approach they may provide an ingredient in defining a UV completion of JT gravity and solve the factorisation problem [34, 35].²

Motivated by this, we consider the computation of multi-boundary partition functions and matter correlation functions in the presence of an EOW brane. While we adopt the techniques developed in [20] and [39] respectively, the modified result we obtain due to the presence of the EOW brane is expected to represent the aforementioned quantities in a single-sided black hole geometry.

Indeed the main concern of the present paper is the computation of the late time behaviour of complexity. We define this as the geodesic length connecting the EOW brane and the asymptotic boundary.³ More concretely, this is calculated in JT gravity as a *quenched expectation value*. The qualitative behaviour remains the same as in the case of a two-sided black hole, namely, the complexity grows linearly at late times up to a time $t \sim e^{S_0}$ and subsequently saturates to a constant value. The value of this constant which is of $\mathcal{O}(e^{S_0})$ depends crucially on the tension of the EOW brane.

Although we adopt the non-perturbative definition⁴ of complexity from [27], we refrain from rewriting it in terms of the correlators as in (1.2). The reason is, although the quantity structurally looks similar to the aforementioned correlators, the limits on Δ appearing in the definition are counter-intuitive and do not agree with the standard geodesic approximation to the two-point function.

Therefore we rather use a modified version of the replica trick in order to compute the quenched expectation value of the length of the geodesic.⁵ This avoids the aforementioned ambiguity. Moreover using the definition of variance engendered by the modified replica approach, we observe time-independent results at late times both for the two-sided and the one-sided geometries. This is in contrast with the result for the variance presented in [27] where the complexity is defined in terms of a two-point function (1.2).

Our paper is organised as follows. We will start by introducing the theory of interest in section 2. By use of the quantisation procedure in the presence of a boundary brane [34], we construct various wavefunctions needed in building up different partition functions and of course the path integral, which describes the volume of the black hole interior for our setting. In this section we also consider matrix elements in the geodesic length basis on the Hilbert space produced by the EOW brane. More specifically, we calculate the off-diagonal elements showing that while we are describing a pure state, they still obey the ETH. In sections 3 and 4 we construct the multi-boundary partition function and the quantum gravity matter correlation functions respectively. We put the pieces together in section 5, where we compute the complexity using the definition mentioned above. Then

²For other approaches to possible non-perturbative completions of JT gravity see [36–38].

³In the Lorentzian picture this replaces the bridge-to-nowhere of [40].

⁴This is non-perturbative by virtue of an analytic continuation of the Euclidean path integral.

⁵Following [27], we only consider non self-intersecting geodesics.

we also consider the variance of this quantity. We conclude in section 6 with a couple of interesting questions and comments on work in progress.

2 Lorentzian JT gravity with EOW Branes and Wavefunctions

In this section we use the canonical quantisation procedure first introduced in [35], to construct different wavefunction expressions for JT gravity in the presence of an EOW brane. After reviewing the quantisation procedure in presence of a boundary brane [34], we generalise the construction to compute wavefunctions for different configurations of the EOW brane on the disk and then for the trumpet. These quantities are the essential building blocks in the calculation of correlation functions as well as complexity in our setup.

2.1 The classical solution

JT gravity is a two-dimensional theory of gravity with the Lorentzian action [15, 16]

$$S_{\text{JT}} = \frac{S_0}{2\pi} \left(\int \sqrt{-g} R + 2 \int \sqrt{|h|} K \right) + \int \sqrt{-g} \phi (R + 2) + 2 \int \sqrt{|h|} \phi (K - 1), \quad (2.1)$$

where the first term is the topological Gauss-Bonnet term and S_0 is the ground state entropy. In addition, we add the action of an EOW brane, which is of the form:

$$S_{\text{Brane}} = \mu \int_{\text{Brane}} ds, \quad (2.2)$$

with μ being the brane tension. In two spacetime dimensions, the eq (2.2) boils down to the action of a particle with mass μ . The overall action is given by

$$S = S_{\text{JT}} + S_{\text{Brane}}. \quad (2.3)$$

The corresponding equations of motion are

$$R + 2 = 0, \quad \nabla_\mu \nabla_\nu \phi - g_{\mu\nu} \nabla^2 \phi + g_{\mu\nu} \phi = 0. \quad (2.4)$$

At the asymptotic AdS boundary, the boundary conditions are set by fixing the induced metric and the dilaton value [17, 18, 41]

$$ds^2|_{\partial M} = -\frac{dt^2}{\epsilon^2}, \quad \phi|_{\partial M} = \frac{\phi_b}{\epsilon}, \quad (2.5)$$

where ϵ is a holographic renormalisation parameter and we are interested in the limit $\epsilon \rightarrow 0$. Additionally, at the EOW brane the following conditions are set [26]

$$K = 0, \quad \partial_n \phi = \mu. \quad (2.6)$$

Here ∂_n denotes the derivative normal to the EOW brane. The latter condition is essential in ensuring dynamical gravity on the EOW brane.

2.2 Quantisation in presence of a brane

Let us denote the normalised geodesic distance between the AdS boundary and the EOW brane by L . The Hilbert space may be constructed in terms of L_2 -normalisable functions of

L .⁶ As the system may be thought of as a particle in a Morse potential, the Hamiltonian amounts to [34]

$$H = \frac{2}{\phi_b} \left(\frac{P^2}{4} + \mu e^{-L} + e^{-2L} \right), \quad (2.7)$$

such that the Schrödinger equation is given by [34, 35]

$$(-\partial_L^2 + 4\mu e^{-L} + 4e^{-2L}) \psi_{\mu,E}(L) = 2E \psi_{\mu,E}(L). \quad (2.8)$$

In going from (2.7) to (2.8) we have set $\phi_b = 1$ and replaced $P \rightarrow -i\partial_L$. In solving (2.8), we are generally assuming $\mu > 0$. Setting $k^2 = 2E$ and $z = 4e^{-L}$ the corresponding normalised wavefunction [34] is⁷

$$\psi_{k,\mu}(z) = \sqrt{f_\mu(k)} \frac{W_{-\mu,ik}(z)}{\sqrt{z}}, \quad \text{with } f_\mu(k) = \gamma_\mu(k)r(k), \quad (2.9)$$

where we have defined

$$\gamma_\mu(k) = \left| \Gamma \left(\frac{1}{2} + \mu + ik \right) \right|^2, \quad r(k) = \frac{k \sinh(2\pi k)}{\pi^2}. \quad (2.10)$$

The normalisation of $\psi_{k,\mu}(z)$ requires the use of the orthogonality relation for Whittaker functions of the second kind of imaginary order [42]

$$\int_0^\infty \frac{dz}{z^2} W_{-\mu,ik}(z) W_{-\mu,ik'}(z) = \frac{1}{f_\mu(k)} \delta(k - k'). \quad (2.11)$$

The quantum mechanical propagator is [34]

$$G_\beta(z_1, z_2) = \langle L_2 | e^{-\beta H} | L_1 \rangle = \int dk e^{-\frac{\beta k^2}{2}} f_\mu(k) \frac{W_{-\mu,ik}(z_1)}{\sqrt{z_1}} \frac{W_{-\mu,ik}(z_2)}{\sqrt{z_2}}. \quad (2.12)$$

Let us now come to a more geometric description in terms of the Euclidean path integral of JT gravity. In the Euclidean picture, the time coordinate τ is periodic with $\tau \sim \tau + \beta$. The Euclidean action is given by

$$S = -\frac{S_0}{2\pi} \left(\int \sqrt{g} R + 2 \int \sqrt{|\hbar|} K \right) - \int \sqrt{g} \phi (R + 2) - 2 \int \sqrt{|\hbar|} \phi (K - 1), \quad (2.13)$$

where we set the following boundary conditions for an asymptotic AdS boundary

$$ds^2|_{\partial M} = \frac{d\tau^2}{\epsilon^2}, \quad \phi|_{\partial M} = \frac{\phi_b}{\epsilon}. \quad (2.14)$$

Again, the first term of (2.13) is purely topological and accounts for the Euler characteristic of the Riemann surface $\chi = 2 - 2g - n$, where g is the genus and n the number of boundaries. The integration over the dilaton localises the path integral to surfaces of con-

⁶This is referred to as the ‘‘L-basis’’ in [35]. The choice of this basis avoids the subtlety of defining a ‘‘time operator’’ whose dual Hamiltonian is bounded from below. Furthermore, this choice also allows for a full phase space \mathbb{R}^2 without any restrictions on the phase space coordinates.

⁷Due to the fact that $W_{a,b} = W_{a,-b}$ we are restricted to $k \geq 0$.

stant negative curvature with an asymptotic boundary length determined by the boundary conditions (2.14). The extrinsic curvature term gives a Schwarzian action to the asymptotic boundary fluctuations on the hyperbolic space [17, 18].

The complete path integral includes an integral over the moduli of such surfaces and the boundary fluctuations. Briefly stated, the higher genus surfaces for one asymptotic boundary may be viewed as consisting of two parts, namely, one asymptotic boundary of fixed length and a geodesic boundary of length b and a remaining genus g Riemann surface with geodesic boundary of the same length b . The genus expansion of JT then takes on the form [20]:

$$\langle Z(\beta) \rangle = e^{S_0} \hat{Z}_D(\beta) + \sum_{g=1} e^{(1-2g)S_0} \int_0^\infty b db V_{g,1}(b) \hat{Z}_T(\beta, b), \quad (2.15)$$

where $V_{g,1}$ is the Weil-Petersson volume of genus g and one geodesic boundary [28, 43] and the integration over b glues the two parts of the surface together. Here $\hat{Z}_D(\beta)$ refers to the disk topology partition function and $\hat{Z}_T(\beta, b)$ to the “trumpet” partition function [20, 44]

$$\hat{Z}_D(\beta) = \frac{e^{\frac{2\pi^2}{\beta}}}{\sqrt{2\pi}\beta^{3/2}}, \quad \hat{Z}_T(\beta, b) = \frac{e^{-\frac{b^2}{2\beta}}}{\sqrt{2\pi}\beta^{1/2}}. \quad (2.16)$$

This construction can be generalised to n asymptotic boundaries with the connected contribution being of the form [20]:

$$\langle Z(\beta_1) \dots Z(\beta_n) \rangle_C = \sum_{g=0} e^{(2-2g-n)S_0} \hat{Z}_{g,n}(\beta_1, \dots, \beta_n), \quad (2.17)$$

with the definition

$$\hat{Z}_{g,n}(\beta_1, \dots, \beta_n) = \int_0^\infty b_1 db_1 \dots b_n db_n V_{g,n}(b_1, \dots, b_n) \hat{Z}_T(\beta_1, b_1) \dots \hat{Z}_T(\beta_n, b_n). \quad (2.18)$$

Moreover, the hats, $\hat{}$ denote quantities without manifest topological weighting. Incorporating the latter, one defines $Z_D(\beta) = e^{S_0} \hat{Z}_D(\beta)$. In our construction, we additionally consider the addition of an EOW brane via the action (2.2) and the boundary conditions (2.6). This modifies the partition function as we explain in the next sections.

At various points we will compute the expectation value of geodesic length in the Euclidean JT path integral. In contrast to the disk, on hyperbolic surfaces of genus $g \geq 1$ there are an infinite number of geodesics. Let us consider the case of non self-intersecting geodesics as in [27]. The moduli space of hyperbolic, bordered Riemann surfaces $\mathcal{M}_{g,n}(b_1, \dots, b_n)$ comes with a symplectic form, the Weil-Petersson form $\Omega = \sum_{i=1}^{3g+n-3} db_i \wedge d\tau_i$, which in principle allows the calculation of the corresponding moduli space volume if restricted to a fundamental domain. Similarly, as first argued for in the $g = 1$ case in [21], and elaborated upon in [27, 45], the integral of the geodesics over moduli space may be calculated by modding via the mapping class group, which we denote $\text{MCG}_{g,n}$. This leads to the expression [21, 27, 27, 28]

$$\int_{\frac{\mathcal{M}_{g,1}}{\text{MCG}_{g,1}}} \Omega \sum_{\gamma} e^{-\Delta \ell_{\gamma}} = e^{-\Delta \ell} \int_{\frac{\mathcal{M}_{g-1,2}}{\text{MCG}_{g-1,2}}} \Omega + \sum_{h \geq 0} e^{-\Delta \ell} \int_{\frac{\mathcal{M}_{h,1}}{\text{MCG}_{h,1}}} \Omega \int_{\frac{\mathcal{M}_{g-h,1}}{\text{MCG}_{g-h,1}}} \Omega. \quad (2.19)$$

This formula may be visualised as cutting along the geodesic and considering the resulting geometries.

2.3 The disk wavefunctions

Let us start by quickly revisiting some results we need from the two-sided AdS system. A natural procedure to prepare the states in the Hilbert space of the two-sided system is via the Hartle- Hawking construction [35], which is depicted in fig.1(a).

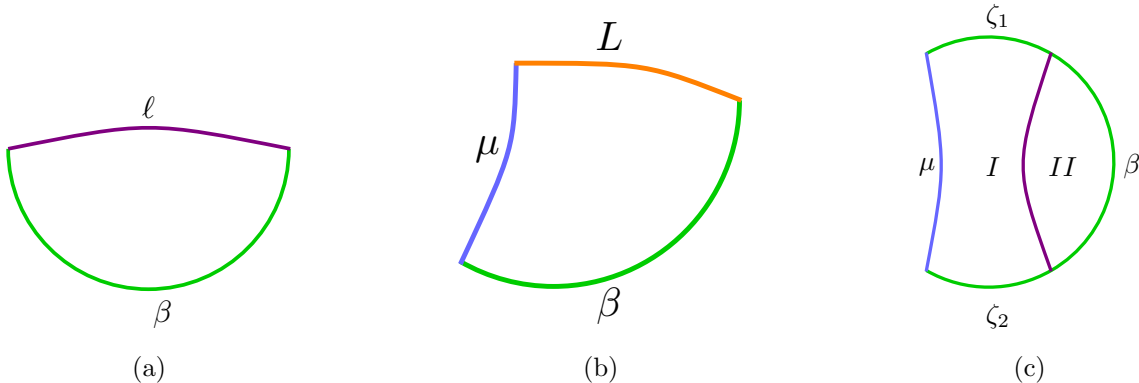


Figure 1: Three possible disk configurations corresponding to different wavefunctions. Figure (a) is the wavefunction of the Hartle-Hawking state of the two-sided AdS system in JT gravity. Figure (b) and figure (c) are two options in the presence of an EOW brane. While in figure (b) we see a geodesic connecting the EOW brane to the asymptotic boundary, for figure (c) the geodesic connects to two different points on the asymptotic boundary. An orange curve corresponds to the former geodesic and a violet curve to the latter. Green denotes an AdS boundary and blue an EOW brane, respectively.

We denote the fixed geodesic length between two parts of the AdS boundary by ℓ . Then the Hartle-Hawking wavefunction $\Phi_{D,\beta}(\ell)$ corresponds to the integral over all Euclidean geometries with disk topology and asymptotic AdS boundary of renormalised length β . Explicitly it amounts to

$$\Phi_D(\beta, \ell) = 2e^{S_0/2} \int_0^\infty dk e^{-\frac{\beta k^2}{2}} r(k) K_{2ik}(y), \quad (2.20)$$

where $y = 4e^{-\frac{\ell}{2}}$. In this formalism the disk partition function is given as

$$\begin{aligned} Z_D(\beta) &= \int_0^\infty \frac{dy}{y} \Phi_D(\beta/2, \ell) \Phi_D(\beta/2, \ell) = \frac{e^{S_0}}{2} \int_0^\infty dk e^{-\frac{\beta k^2}{2}} r(k) \\ &= e^{S_0} \int_0^\infty dE e^{-\beta E} \hat{\rho}_D(E), \end{aligned} \quad (2.21)$$

where $\hat{\rho}_D(E)$ is the disk density of states, which is given as [39, 44, 46–49]

$$\hat{\rho}_D(E) = \frac{\sinh(2\pi\sqrt{2E})}{2\pi^2}. \quad (2.22)$$

From (2.21) we see that the wavefunction is normalised in such a way to give the correct expression for (2.21) and (2.22).

Before moving on to more complicated hyperbolic surfaces, let us now introduce the EOW brane already in this setting and construct the disk wavefunction in its presence. We can interpret the resulting wavefunction as the Hartle-Hawking wavefunction in the L basis for the case of a one-sided black hole. This wavefunction is associated to a region enclosed by an asymptotically AdS boundary of renormalised length β , an EOW brane and a geodesic of length L connecting them.⁸ This configuration is depicted in fig.1(b).

We will denote the corresponding wavefunction by $\Psi_D(\beta, L)$ ⁹ which should satisfy

$$\int_0^\infty \frac{dz}{z} \Psi_D(\beta/2, L) \Psi_D(\beta/2, L) = \int_0^\infty \frac{dz_1}{z_1} \frac{dz_2}{z_2} \Psi_D(x, L_1) G_{\beta-2x}(z_1, z_2) \Psi_D(x, L_2), \quad (2.23)$$

where the variable of integration is $z = 4e^{-L}$. It is straightforward to see that (2.23) is fulfilled for the following expression

$$\Psi_D(\beta, L) = \frac{e^{S_0/2}}{\sqrt{2}} \int_0^\infty dk e^{-\frac{\beta k^2}{2}} \gamma_\mu(k) r(k) \frac{W_{-\mu, ik}(z)}{\sqrt{z}}. \quad (2.24)$$

The disk partition function in the presence of an EOW brane therefore amounts to

$$\begin{aligned} Z_{D,\mu}(\beta) &= \int_0^\infty \frac{dz}{z} \Psi_D(\beta/2, L) \Psi_D(\beta/2, L) = \frac{e^{S_0}}{2} \int_0^\infty dk e^{-\frac{\beta k^2}{2}} \gamma_\mu(k) r(k) \\ &= e^{S_0} \int_0^\infty dE e^{-\beta E} \gamma_\mu(E) \hat{\rho}_D(E), \end{aligned} \quad (2.25)$$

Comparing (2.25) to (2.21) we see that the effect of the EOW brane is encompassed by an additional Γ -function expression defined in (2.10). The above expressions also allow us to calculate the wavefunction $\Psi_D(\zeta_1, \zeta_2, \ell)$ for region I depicted in fig. 1(c): a region enclosed by an EOW brane and a geodesic connecting points on the asymptotic AdS boundary. This wavefunction can be derived from the identification,

$$Z_{D,\mu}(\beta) = \int_0^\infty \frac{dy}{y} \Psi_D(\zeta_1, \zeta_2, \ell) \Phi_D(\beta - \zeta_1 - \zeta_2, \ell), \quad (2.26)$$

by which, using (2.20), one arrives at

$$\Psi_D(\zeta_1, \zeta_2, \ell) = 2e^{S_0/2} \int_0^\infty dk e^{-\frac{k^2}{2}(\zeta_1+\zeta_2)} \gamma_\mu(k) r(k) K_{2ik}(y). \quad (2.27)$$

2.4 The trumpet wavefunctions

The most important ingredients of our study are the wavefunctions on the trumpets whose asymptotic boundaries are either pinched off by the disk regions considered in fig.1 or replaced in some parts by the EOW brane.

While more complicated hyperbolic surfaces require the use of Riemann surfaces with geodesic boundaries, the simplest configuration on the trumpet is depicted in fig. 2(a).

⁸In contrast to the geodesic length connecting two points on the AdS boundary which we denoted by ℓ .

⁹We denote wavefunctions associated to the two-sided black hole via Φ and those in the presence of EOW branes by Ψ .

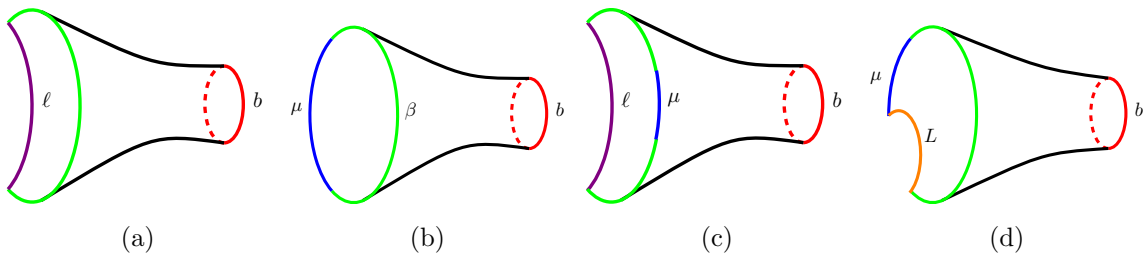


Figure 2: Four different possible trumpet geometries corresponding to four distinct wavefunctions. The closed geodesic boundary is depicted in red. In figure (a) we see the generalisation of the disk configuration, figure 1(a) to the trumpet. Figure (b) corresponds to the wavefunction on a trumpet geometry with both an EOW brane and an asymptotically AdS boundary. Figure (c) shows the wavefunction of a geodesic connecting two points on an asymptotically AdS boundary which contains an EOW brane. Lastly, in figure (d) we see a geodesic connecting EOW brane and AdS boundary on a trumpet geometry.

The corresponding wavefunction $\Phi_T(\beta, b, \ell)$ can be realised as the trumpet wavefunction pinched off by the disk wavefunction shown in fig. 1(a). This is obtained through the identity

$$\Phi_T(\beta, b) = \frac{1}{\pi} \int_0^\infty dk \cos(kb) e^{-\frac{\beta k^2}{2}} = \int_0^\infty \frac{dy}{y} \Phi_T(\beta - x, b, \ell) \Phi_D(x, \ell), \quad (2.28)$$

which results in

$$\Phi_T(\beta, b, \ell) = \frac{4e^{-S_0/2}}{\pi} \int_0^\infty dk e^{-\frac{\beta k^2}{2}} \cos(kb) K_{2ik}(y). \quad (2.29)$$

Let us now come to the geometry depicted in fig.2(b). This can be computed by gluing the above geometry with a region enclosed by a geodesic and EOW brane as shown in fig.1(c). This yields the wavefunction $\Psi_T(\beta, b)$ associated with this diagram

$$\Psi_T(\beta, b) = \int_0^\infty \frac{dy}{y} \Phi_T(\beta, b, \ell) \Psi_D(0, 0, \ell) = \frac{1}{\pi} \int_0^\infty dk \cos(kb) \gamma_\mu(k) e^{-\frac{\beta k^2}{2}}. \quad (2.30)$$

The wavefunction (2.30) is in a perfect agreement with the corresponding wavefunction presented in [34].

This in turn allows for the calculation of $\Psi_T(\zeta_1, \zeta_2, b, \ell)$, the wavefunction associated with fig.2(c) and obtained through the equation

$$\Psi_T(\beta, b) = \int_0^\infty \frac{dy}{y} \Psi_T(\zeta_1, \zeta_2, b, \ell) \Phi_D(\beta - \zeta_1 - \zeta_2, \ell). \quad (2.31)$$

Using (2.20) and (2.30), this yields

$$\Psi_T(\zeta_1, \zeta_2, b, \ell) = \frac{4e^{-S_0/2}}{\pi} \int_0^\infty dk \cos(kb) \gamma_\mu(k) e^{-\frac{k^2}{2}(\zeta_1 + \zeta_2)} K_{2ik}(y). \quad (2.32)$$

Finally, the wavefunction corresponding to the geometry shown in the panel (d) of fig.

2, namely a trumpet geometry with geodesic of length L from the EOW brane to the asymptotic boundary, can be computed by pinching-off the wavefunction $\Psi_D(\beta, L)$ from the above wavefunction. Therefore the structure

$$\Psi_T(\beta, b) = \int_0^\infty \frac{dz}{z} \Psi_T(\beta - x, b, L) \Psi_D(x, L), \quad (2.33)$$

by use of (2.24) results in the wavefunction

$$\Psi_T(\beta, b, L) = \frac{\sqrt{2}e^{-S_0/2}}{\pi} \int_0^\infty dk \cos(kb) \gamma_\mu(k) e^{-\frac{\beta k^2}{2}} z^{-1/2} W_{-\mu, ik}(z). \quad (2.34)$$

2.5 Pure vs. Thermal States

As already mentioned in the introduction, by considering an EOW brane we are describing a pure state. However, to establish its interpretation as a typical boundary state, it is essential to try and delineate differences to a thermal state. We can check the expectation value of the energy. Indeed at disk level this amounts to

$$\langle E \rangle = \frac{\int_0^\infty \frac{dz}{z} \Psi_D(\beta/2, L) H \Psi_D(\beta/2, L)}{\int_0^\infty \frac{dz}{z} \Psi_D(\beta/2, L) \Psi_D(\beta/2, L)}, \quad (2.35)$$

with H being the Hamiltonian defined in (2.7). As the corresponding system may be thought of as a particle in a Morse potential, by use of the Schrödinger equation, one arrives at

$$\langle E \rangle = -\frac{\partial}{\partial \beta} \ln Z_\mu(\beta), \quad (2.36)$$

which is in agreement with the expectation value of a thermal ensemble with temperature $\frac{1}{\beta}$. This may be readily generalised to higher genus. Therefore the wavefunctions in the presence of an EOW brane indeed correspond to states which are indistinguishable from thermal states.

On the other hand we note that the ETH delineates between diagonal and off-diagonal matrix elements. More explicitly, the matrix elements of observables in the eigenstate of the Hamiltonian are given by [50]

$$\mathcal{O}_{mn} = \mathcal{O}(\bar{E})\delta_{mn} + e^{-\frac{S(\bar{E})}{2}} f_{\mathcal{O}}(\bar{E}, \omega) R_{mn}, \quad (2.37)$$

where $\bar{E} = \frac{E_m + E_n}{2}$, $\omega = E_m - E_n$ and $S(\bar{E})$ is the entropy. Moreover, $\mathcal{O}(\bar{E})$ is the expectation value in the microcanonical ensemble, $f_{\mathcal{O}}(\bar{E}, \omega)$ is a smooth function and R_{mn} a random variable with zero mean and unit variance.

One observes that off-diagonal elements are suppressed by the Hilbert space size. In order to show that the wavefunction we consider also satisfies ETH, we need to calculate off-diagonal elements of the inner product in the length basis $|L\rangle$ used in the quantisation of (2.7). Actually the inner product we need for this analysis was already considered in [34], where the importance of higher topologies was stressed. First we need to define a building block, which is shown in fig.3. Denoting the corresponding wavefunction by $\Psi_T(b, L_1, L_2)$, one has

$$\Psi_T(\beta, b) = \int_0^\infty \frac{dz_1}{z_1} \frac{dz_2}{z_2} \Psi_D(\beta - x, L_1) \Psi_T(b, L_1, L_2) \Psi_D(x, L_2), \quad (2.38)$$

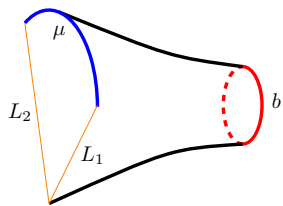


Figure 3: One important ingredient in the calculation of the leading order correction to the inner product $\langle L_1|L_2\rangle$ via Euclidean path integral. We see the two geodesics L_1 and L_2 in orange, the EOW brane in blue and a closed geodesic b in red. The wavefunction of this geometry is denoted by $\Psi_T(b, L_1, L_2)$. Topologies beyond the disk are important in recovering ETH-like behaviour.

which in combination with the expression (2.24) may be used to find

$$\Psi_T(b, L_1, L_2) = \frac{2e^{-S_0}}{\pi} \int_0^\infty dk \cos(kb) \gamma_\mu(k) (z_1 z_2)^{-1/2} W_{-\mu, ik}(z_1) W_{-\mu, ik}(z_2), \quad (2.39)$$

in agreement with the result obtained in [34]. The wavefunction (2.39) plays an important role in recovering ETH behaviour, as the standard canonical quantisation condition

$$\langle L_1|L_2\rangle = \delta(L_1 - L_2), \quad (2.40)$$

is corrected via higher genus contributions to the expression

$$\langle L_1|L_2\rangle = \delta(L_1 - L_2) + \int_0^\infty b db X(b) \Psi_T(b, L_1, L_2), \quad (2.41)$$

where we have introduced the notation $X(b)$ as in [34]. Here $X(b)$ is an integration measure which corresponds to all topologies ending on a single closed geodesic length b , such that the weighting by the Euler characteristic and the Weil-Petersson volumes are included in this quantity. We could also consider it to include an arbitrary number of EOW brane loops as in [34]. By use of (2.39), (2.41) takes on the form

$$\langle L_1|L_2\rangle = \delta(L_1 - L_2) + \frac{2e^{-S_0}}{\pi} \int_0^\infty dk \chi(k) \gamma_\mu(k) \frac{W_{-\mu, ik}(z_1) W_{-\mu, ik}(z_2)}{\sqrt{z_1 z_2}}, \quad (2.42)$$

where

$$\chi(k) = \int_0^\infty b db X(b) \cos(kb). \quad (2.43)$$

The leading contribution to the off-diagonal term comes from surfaces with genus one for which $\chi(k) \sim e^{-S_0}$, which results in

$$\langle L_1|L_2\rangle \approx \delta(L_1 - L_2) + (\dots)_{L_1, L_2} e^{-2S_0}, \quad (2.44)$$

in agreement with [51]. Here $(\dots)_{L_1, L_2}$ refers to the $g = 1$ contribution, where we have already pulled out the topological weighting. We therefore see that off-diagonal terms are suppressed exponentially just as in (2.37).

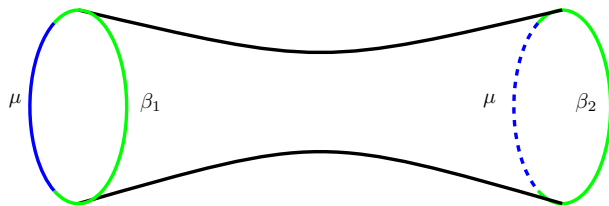


Figure 4: Two trumpet geometries glued together along their closed geodesic boundaries. This geometry corresponds to the connected part of the spectral form factor.

3 Partition Function

In this section we construct the partition function in the presence of an EOW brane via the wavefunction formalism developed in section 2. The most natural quantity to analyse is the two-point function or the spectral form factor. More specifically, we require the trumpet wavefunction (2.30). We may visualise the connected contribution to the two-point function as gluing two trumpet geometries of the type illustrated in fig.2(a) together along their closed geodesic boundaries, which results in the geometry shown in fig.4.

In analogy to (2.17), the overall contribution including connected and disconnected structures gives the following expression:

$$\begin{aligned}
& \langle Z(\beta_1)Z(\beta_2) \rangle_\mu \\
&= \int_0^\infty b_1 db_1 \int_0^\infty b_2 db_2 \Psi_T(\beta_1, b_1) X(b_1, b_2) \Psi_T(\beta_2, b_2) \\
&= \frac{e^{-S_0}}{\pi^2} \int_0^\infty dk_1 dk_2 e^{-\frac{\beta_1 k_1^2}{2} - \frac{\beta_2 k_2^2}{2}} \gamma_\mu(k_1) \gamma_\mu(k_2) \int_0^\infty b_1 db_1 \int_0^\infty b_2 db_2 X(b_1, b_2) \cos(k_1 b_1) \cos(k_2 b_2).
\end{aligned} \tag{3.1}$$

Here we have introduced the function $X(b_1, b_2)$ that denotes the topologically weighted sum over the Weil-Petersson volumes associated to surfaces with two geodesic boundaries parametrised by b_1 and b_2 . It is of the form

$$X(b_1, b_2) := \sum_{g=0} e^{(2-2g)S_0} \left(V_{g-1,2}(b_1, b_2) + \sum_{a \geq 0} V_{g-a,1}(b_1) V_{a,1}(b_2) \right). \tag{3.2}$$

We note that the first term of (3.2) corresponds to the connected contribution, whereas the second term corresponds to the disconnected contribution. There are two contributions in (3.1) which must be put in “by hand” as the moduli space volumes $V_{g=0,1}(b)$ and $V_{g=0,2}(b_1, b_2)$ in (3.2) are undefined.¹⁰ For the disconnected contributions involving $V_{g=0,1}(b)$, the correct result is given by (2.25) and the two boundary $g = 0$ connected contribution is defined as

$$Z(\beta_1, \beta_2)_{g=0, n=2, \mu} = \int_0^\infty b_1 db_1 \int_0^\infty b_2 db_2 \Psi_T(\beta_1, b_1) \Psi_T(\beta_2, b_2). \tag{3.3}$$

Comparing (3.1) to the two-sided expression of [20], one observes that the distinction to

¹⁰These two volumes constitute input values for the topological recursion [52, 53].

(3.1) lies in the factor $\gamma_\mu(k_1)\gamma_\mu(k_2)$. Analytically continuing (3.1) to the spectral form factor and rewriting in terms of energy variables one arrives at

$$\langle Z(\beta + it)Z(\beta - it) \rangle_\mu = \int_0^\infty dE_1 dE_2 e^{-\beta(E_1+E_2)-it(E_1-E_2)} \gamma_\mu(E_1)\gamma_\mu(E_2) \langle \rho(E_1)\rho(E_2) \rangle \quad (3.4)$$

where

$$\langle \rho(E_1)\rho(E_2) \rangle = \int b_1 db_1 b_2 db_2 X(b_1, b_2) \frac{\cos(b_1\sqrt{2E_1})\cos(b_2\sqrt{2E_2})}{2\pi^2\sqrt{E_1E_2}}, \quad (3.5)$$

which is the density of states corresponding to two boundary case of (2.17). At late times, the integral (3.4) is dominated by small energy ranges, and it can be shown that for $|E_1 - E_2| \ll 1$, non-perturbative contributions give the following expression for (3.5)[20]¹¹

$$\langle \rho(E_1)\rho(E_2) \rangle \approx e^{2S_0} \hat{\rho}_D(E_1)\hat{\rho}_D(E_2) + e^{S_0} \hat{\rho}_D(E_2)\delta(E_1 - E_2) - \frac{\sin^2(\pi e^{S_0} \hat{\rho}_D(E_2)(E_1 - E_2))}{\pi^2(E_1 - E_2)^2}, \quad (3.6)$$

where $\hat{\rho}_D(E)$ refers to the genus zero contribution to the density of states (2.22). The last term in (3.6) is the so-called sine-kernel. The non-perturbative nature of this contribution can be spotted by noting the factor of e^{S_0} inside the “sin”. As should be expected, plugging (3.6) into (3.4), gives a ramp-plateau structure for the connected and decaying behaviour for the disconnected contribution.

4 Correlation Functions

Following the procedure of [39] we will now determine full quantum gravity expressions for the matter correlation functions in the presence of an EOW brane. The idea of [39] is to construct a certain Kernel which can be used to dress quantum field theory correlation functions on AdS₂ to produce gravity correlators. For the two-sided case, the Kernel essentially amounts to the Hartle-Hawking wavefunction (2.20). More concretely, let us denote the coordinates by $\mathbf{x} = (\xi, x)$, where ξ is the holographic coordinate and x the boundary coordinate. The regularised geodesic distance between two points is given by

$$e^{\frac{\ell}{2}} = \frac{|x_1 - x_2|}{\sqrt{\xi_1\xi_2}}. \quad (4.1)$$

In terms of this expression the Kernel is

$$K(u_{12}, \mathbf{x}_1, \mathbf{x}_2) = 2e^{S_0/2} \frac{4\sqrt{\xi_1\xi_2}}{|x_1 - x_2|} \int_0^\infty dk e^{-\frac{u_{12}k^2}{2}} r(k) K_{2ik} \left(\frac{4\sqrt{\xi_1\xi_2}}{|x_1 - x_2|} \right). \quad (4.2)$$

The quantum gravity correlators constructed in [39] then amount to

$$\langle \mathcal{O}_1(u_1) \cdots \mathcal{O}_n(u_n) \rangle_D = \int_{x_1 > \cdots > x_n} \frac{\prod_i d\xi_i dx_i}{\text{Vol}(\text{SL}(2, R))} K(u_{12}, \mathbf{x}_1, \mathbf{x}_2) \cdots K(u_{1n}, \mathbf{x}_n, \mathbf{x}_1) \quad (4.3)$$

$$\times \prod_i \xi_i^{\Delta_i - 2} \langle \mathcal{O}_1(x_1) \cdots \mathcal{O}_n(x_n) \rangle_{\text{CFT}},$$

¹¹See also [22] based on the elegant approach of [54, 55].

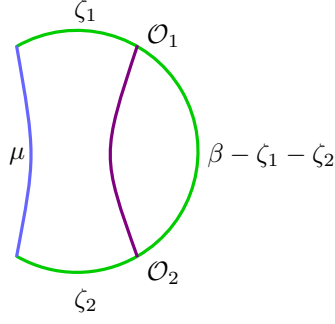


Figure 5: This figure corresponds to the two-point function of two operators \mathcal{O}_1 and \mathcal{O}_2 on the Euclidean disk in the presence of an EOW brane. The corresponding wavefunction is given in (2.27).

where Δ_i is the scaling dimension of the operator \mathcal{O}_i . $\text{Vol}(\text{SL}(2, R))$ reminds us that one needs to fix the $\text{SL}(2, R)$ gauge symmetry. In our case, while the general logic leading to the structure of (4.3) is preserved, now two different Kernels have to be used. In addition to (4.2), a Kernel must be introduced due to the presence of the EOW brane. A quick look at fig.5 suggests that this Kernel corresponds to the wavefunction (2.27), which results in the expression

$$M(\zeta_1, \zeta_2, \mathbf{x}_1, \mathbf{x}_2) = 2e^{S_0/2} \frac{4\sqrt{\xi_1\xi_2}}{|x_1 - x_2|} \int_0^\infty dk e^{-\frac{k^2}{2}(\zeta_1 + \zeta_2)} \gamma_\mu(k) r(k) K_{2ik} \left(\frac{4\sqrt{\xi_1\xi_2}}{|x_1 - x_2|} \right). \quad (4.4)$$

Using this kernel and (4.2) the quantum gravity correlators in the presence of an EOW brane is

$$\begin{aligned} \langle \mathcal{O}_1(u_1) \cdots \mathcal{O}_n(u_n) \rangle_{D, \mu} &= \int_{x_1 > \dots > x_n} \frac{\prod_i d\xi_i dx_i}{\text{Vol}(\text{SL}(2, R))} K(u_{12}, \mathbf{x}_1, \mathbf{x}_2) \cdots K(u_{n-1n}, \mathbf{x}_{n-1}, \mathbf{x}_n) \\ &\times M(\zeta_1, \zeta_n, \mathbf{x}_n, \mathbf{x}_1) \prod_i \xi_i^{\Delta_i - 2} \langle \mathcal{O}_1(x_1) \cdots \mathcal{O}_n(x_n) \rangle_{\text{CFT}}. \end{aligned} \quad (4.5)$$

The above expressions are for disk topology as indicated by the index D . Let us briefly describe how to generalise to arbitrary topology by use of the two-point function as a concrete example. For the disk the two-point function is shown in fig.5. The variables of fig.5 are related to those of formula (4.5) via $u = \zeta_1 + \zeta_2$. Keeping in mind that the CFT two-point function is given by:

$$\langle \mathcal{O}_1(x_1) \mathcal{O}_2(x_2) \rangle = e^{-\Delta \ell}, \quad (4.6)$$

we arrive at the quantum gravity two-point function at disk level (according to (4.5))

$$\begin{aligned} \langle \mathcal{O}_1(\zeta_1 + \zeta_2) \mathcal{O}_2(0) \rangle_{D, \mu} &= \int_0^\infty \frac{dy}{y} \Phi_D(\beta - \zeta_1 - \zeta_2, \ell) \Psi_D(\zeta_1, \zeta_2, \ell) \left(\frac{y}{4} \right)^{2\Delta} \\ &= e^{S_0} \int_0^\infty dk_1 dk_2 e^{-\frac{k_1^2}{2}(\beta - u) - \frac{k_2^2}{2}u} r(k_1) r(k_2) \gamma_\mu(k_2) \mathcal{N}(\Delta, k_1, k_2), \end{aligned} \quad (4.7)$$

where

$$\mathcal{N}(\Delta, k_1, k_2) = 4 \int_0^\infty \frac{dy}{y} K_{2ik_1}(y) K_{2ik_2}(y) \left(\frac{y}{4}\right)^{2\Delta} = \frac{|\Gamma(\Delta + i(k_1 + k_2))\Gamma(\Delta + i(k_1 - k_2))|^2}{2^{2\Delta+1}\Gamma(2\Delta)}. \quad (4.8)$$

Comparing (4.7) to the expression for the two-sided AdS black hole [39] we again see the new factor $\gamma_\mu(k)$ due to the presence of the EOW brane.

In order to generalise (4.7) to higher genus, the wavefunctions (2.29) and (2.32) are needed. By making use of these wavefunctions and formula (2.19) the two-point function of arbitrary genus is

$$\begin{aligned} \langle \mathcal{O}_1(\zeta_1 + \zeta_2)\mathcal{O}_2(0) \rangle_\mu &= \int b_1 db_1 b_2 db_2 X(b_1, b_2) \quad (4.9) \\ &\quad \times \int_0^\infty \frac{dy}{y} \Phi_T(\beta - \zeta_1 - \zeta_2, b_1, \ell) \Psi_T(\zeta_1, \zeta_2, b_2, \ell) \left(\frac{y}{4}\right)^{2\Delta} \\ &= \frac{16e^{-S_0}}{\pi^2} \int_0^\infty dk_1 dk_2 \gamma_\mu(k_2) e^{-\frac{k_1^2}{2}(\beta-u) - \frac{k_2^2}{2}u} \mathcal{N}(\Delta, k_1, k_2) \\ &\quad \times \int b_1 db_1 b_2 db_2 X(b_1, b_2) \cos(k_2 b_2) \cos(k_1 b_1). \end{aligned}$$

We note, however, that the disk contribution is a particular case and it is understood that the genus zero contribution is defined to be (4.7). Altogether one gets

$$\langle \mathcal{O}_1(u)\mathcal{O}_2(0) \rangle_\mu = 16e^{-S_0} \int_0^\infty dE_1 dE_2 e^{-E_1(\beta-u) - E_2 u} \gamma_\mu(E_2) \langle \rho(E_1)\rho(E_2) \rangle \mathcal{N}(\Delta, E_1, E_2), \quad (4.10)$$

where we are using (3.5). The late-time behaviour of the two-point function amounts to considering the analytic continuation $u = \beta + it$, which gives

$$\langle \mathcal{O}_1(t)\mathcal{O}_2(0) \rangle_\mu = 16e^{-S_0} \int_0^\infty dE_1 dE_2 e^{-\frac{\beta}{2}(E_1+E_2) + it(E_1-E_2)} \gamma_\mu(E_2) \langle \rho(E_1)\rho(E_2) \rangle \mathcal{N}(\Delta, E_1, E_2). \quad (4.11)$$

Comparing this expression to (3.4) shows that the late-time behaviour is essentially the same as that of spectral form factor. Indeed as far as the ramp and the plateau are concerned the extra $\mathcal{N}(\Delta, E_1, E_2)$ plays no essential role.

5 The late time behaviour of complexity

In this section we would like to study the late time behaviour of complexity in our setup. It is conjectured that the holographic quantum complexity is given by the volume of the Einstein-Rosen bridge [6]. In our language in two dimensions it translates into the length of a geodesic connecting two boundaries. This definition was used to compute the late time behaviour of complexity of a two-sided black hole in [27]. In that work it was shown that the complexity exhibits linear growth at late times before it eventually saturates to a finite value. As detailed in the introduction, the most essential step in this construction was the use of the non-perturbative expression (3.6) to furnish the saturation at late times.

In this section we adopt the same logic to work out the late time behaviour of complexity for a single-sided black hole. Crucially however, we do not relate the geodesic length to a matter two-point function but use the quenched expectation value. For the calculation

of the complexity itself this leads to the same expressions for the two-sided case but a decisively different result for the variance. For the one-sided case, we need to compute the quenched expectation value of a geodesic suspended between the AdS boundary and the EOW brane. Note that, in our notation, classically the geodesic distance between boundary and EOW brane is denoted by $L = -\ln z/4$. The complexity is therefore proportional to the expectation value of the geodesic $\mathcal{C} \sim \langle L \rangle_{QG}$ in quantum gravity. It is also worth noting that in the present case one could also compute the expectation value of a geodesic length connecting two points on the boundary, $\langle \ell \rangle_{QG}$. In what follows we will study the time dependence of these quantities using the wavefunction formalism we developed in the previous sections.

5.1 The geodesic ℓ

To proceed, let us start with the geodesic ℓ which is used in the two-sided case and compute its “quantum expectation” value. At the disk level one has

$$\langle \ell(u) \rangle = -\frac{1}{Z_{D,\mu}(\beta)} \int_0^\infty \frac{dy}{y} \Psi_D(\zeta_1, \zeta_2, \ell) \Phi_D(\beta - u, \ell) \left(2 \ln \frac{y}{4}\right), \quad \text{with } u = \zeta_1 + \zeta_2. \quad (5.1)$$

To evaluate this quantity, we will use a trick which is inspired by the replica trick used *e.g.* in computing the quenched free energy. We write the logarithm in terms of the following limit¹²

$$\ln A = \lim_{N \rightarrow 0} \frac{A^N - 1}{N} = \lim_{N \rightarrow 0} \frac{d}{dN} A^N. \quad (5.2)$$

We normalise by multiplying with a factor of $Z_{D,\mu}^{-1}(\beta)$, where $Z_{D,\mu}(\beta)$ is the disk partition function, given in (2.25). Using this definition one may define complexity as

$$\langle \ell(u) \rangle = -\lim_{N \rightarrow 0} \frac{\langle y^{2N} \rangle_u - 1}{N}, \quad (5.3)$$

where

$$\langle y^{2N} \rangle_u = \frac{1}{Z_{D,\mu}(\beta)} \int_0^\infty \frac{dy}{y} \Psi_D(\zeta_1, \zeta_2, \ell) \Phi_D(\beta - u, \ell) \left(\frac{y}{4}\right)^{2N} \quad (5.4)$$

and it is understood that an analytic continuation must still be performed. Expressions such as (5.4) may then be calculated via (2.19). It is very interesting that in this context, the complexity, similar to entanglement entropy, can also be computed via a replica trick. To be clear, while the expression (5.4) is calculated in the Euclidean path integral, we have not explicitly shown the existence of replicated geometries. Perhaps one should take the validity of (5.4) as an indication on the existence of some kind of broader approach involving replica geometries. It is also worth noting that the above expression found by use of a replica trick is identical to the expression of the matter two-point function (4.7) with the identification of $\Delta = N$. However, although they are the same expression, conceptually they play different roles as (5.4) is used in (5.3). This is where our approach deviates significantly from [27].

Indeed, it is not clear if one could interpret (5.4) as a matter two-point function since the corresponding matter two-point function is obtained from an opposite limit, namely, in the limit of large scaling dimension. On the contrary, in our case, we need the limit, $N \rightarrow 0$

¹²In the context of JT gravity, see [56–59].

by which we lose the semiclassical interpretation of the two-point function. Nonetheless, as long as the computations are concerned, both yield the same result.

In particular from (4.7) by use of (2.19) one gets

$$\langle y^{2N} \rangle_u = \frac{e^{S_0}}{Z_{D,\mu}(\beta)} \int_0^\infty dk_1 dk_2 e^{-\frac{k_1^2}{2}(\beta-u) - \frac{k_2^2}{2}u} r(k_1)r(k_2) \gamma_\mu(k_2) \mathcal{N}(N, k_1, k_2). \quad (5.5)$$

Of course this expression in itself does not yet furnish late time linear growth as (5.5) is not the end of the story and needs to be plugged into the replica formula (5.3) and analytically continued to find complexity. Performing the analytic continuation $u = \frac{\beta}{2} + it$ and using energy variables we arrive at

$$\langle y^{2N} \rangle_t = \frac{e^{S_0}}{Z_{D,\mu}(\beta)} \int_0^\infty dE_1 dE_2 e^{-\frac{\beta}{2}(E_1+E_2) + i(E_1-E_2)t} \hat{\rho}_D(E_1)\hat{\rho}_D(E_2) \gamma_\mu(E_2) \mathcal{N}(N, E_1, E_2). \quad (5.6)$$

Now we have to simply plug this equation into the replica formula (5.3). Moreover since we are interested in the behaviour at late times, the main contribution should come from the coincident limit, $E_1 \rightarrow E_2$. In this limit, using the change of variables,

$$E = \frac{E_1 + E_2}{2}, \quad \omega = E_1 - E_2, \quad (5.7)$$

one gets

$$\langle \ell(t) \rangle \sim \text{const.} - \frac{e^{S_0}}{2\sqrt{2\pi}Z_{D,\mu}(\beta)} \int_0^\infty dE e^{-\beta E} \sqrt{E} \hat{\rho}_D(E) \gamma_\mu(E) \int_{-\infty}^\infty d\omega \frac{e^{i\omega t}}{\omega^2}, \quad (5.8)$$

which results in the linear growth $\langle \ell(t) \rangle \sim t$. Of course, one still needs to perform the integral over E , though we will not do it here. Here our aim was only to show that the linear growth at the disk level could be thought of as the consequence of our replica trick. Performing the calculation of the quenched length on a two-boundary topology and using (3.6) would lead to the results already obtained in [27] and we will therefore not do this explicitly.

5.2 The geodesic L

It is straightforward to compute the late time behaviour of the quantum expectation value of the length of the geodesic connecting a point on the boundary to one on the EOW brane

$$\langle L(u) \rangle = -\frac{1}{Z_{D,\mu}(\beta)} \int_0^\infty \frac{dz}{z} \Psi_D(\beta - u, L) \Psi_D(u, L) \ln \frac{z}{4} = -\lim_{N \rightarrow 0} \frac{\langle z^N \rangle_u - 1}{N}, \quad (5.9)$$

where

$$\begin{aligned} \langle z^N \rangle_u &= \frac{1}{Z_{D,\mu}(\beta)} \int_0^\infty \frac{dz}{z} \Psi_D(\beta - u, L) \Psi_D(u, L) \left(\frac{z}{4}\right)^N \\ &= \frac{e^{S_0}}{2Z_{D,\mu}(\beta)} \int_0^\infty dk_1 dk_2 e^{-\frac{k_1^2}{2}(\beta-u) - \frac{k_2^2}{2}u} \gamma_\mu(k_1)\gamma_\mu(k_2)r(k_1)r(k_2) \mathcal{M}(N, k_1, k_2). \end{aligned} \quad (5.10)$$

Here we have introduced

$$\mathcal{M}(N, k_1, k_2) = \int_0^\infty \frac{dz}{z^2} W_{-\mu, ik_1}(z) W_{-\mu, ik_2}(z) \left(\frac{z}{4}\right)^N. \quad (5.11)$$

At this point, one could perform a computation similar to what was done in the case of $\langle \ell(u) \rangle$ in the previous section to find the late time behavior of $\langle L(u) \rangle$. In general, we would expect to get the same linear growth as before, although in this case we will have to deal with the Whittaker functions. However, we will postpone this computation for a little while and will first study the higher genus corrections to the late time behaviour of complexity. The reason for changing the order of computation is as follows. The computation of complexity as the quantum expectation value of the geodesic length at the disk level yields a late time linear growth which keeps growing forever. However, on general grounds it is expected that complexity saturates at late times. Therefore the disk level computation should not constitute the entire story. It is natural to expect that the inclusion of higher topologies and connected geometries plays an important role. Thus, in order to see the saturation phase, one needs to compute the quantum expectation of geodesic length taking into account surfaces of higher genus [27]. By making use of the trumpet wavefunctions we have found in section 2.4, one has

$$\langle L(u) \rangle = -\frac{1}{Z_\mu(\beta)} \int b_1 db_1 b_2 db_2 X(b_1, b_2) \int_0^\infty \frac{dz}{z} \Psi_T(\beta - u, b_1, L) \Psi_T(u, b_2, L) \ln \frac{z}{4}, \quad (5.12)$$

where we have used the notation (3.2) again. In this case we compute the following quantity to be used in the replica formula

$$\langle z^N \rangle_u = \frac{1}{Z_\mu(\beta)} \int b_1 db_1 b_2 db_2 X(b_1, b_2) \int_0^\infty \frac{dz}{z} \Psi_T(\beta - u, b_1, L) \Psi_T(u, b_2, L) \left(\frac{z}{4}\right)^N. \quad (5.13)$$

Using equation (2.34) and expression (5.11) one finds

$$\begin{aligned} \langle z^N \rangle_u &= \frac{2e^{-S_0}}{\pi^2 Z_\mu(\beta)} \int_0^\infty dk_1 dk_2 e^{-\frac{k_1^2}{2}(\beta-u) - \frac{k_2^2}{2}u} \gamma_\mu(k_1) \gamma_\mu(k_2) \\ &\quad \times \int b_1 db_1 b_2 db_2 X(b_1, b_2) \cos(k_1 b_1) \cos(k_2 b_2) \mathcal{M}(N, k_1, k_2), \end{aligned} \quad (5.14)$$

which in the energy variable may be reexpressed as

$$\langle z^N \rangle_u = \frac{2e^{-S_0}}{Z_\mu(\beta)} \int_0^\infty dE_1 dE_2 e^{-E_1(\beta-u) - E_2 u} \gamma_\mu(E_1) \gamma_\mu(E_2) \langle \rho(E_1) \rho(E_2) \rangle \mathcal{M}(N, E_1, E_2), \quad (5.15)$$

$\langle \rho(E_1) \rho(E_2) \rangle$ being the spectral correlation. The main part of the above equation is $\mathcal{M}(N, E_1, E_2)$ which is an integral involving Whittaker functions. This can be evaluated

using the integral identity [60]

$$\begin{aligned}
\int_0^\infty x^{\rho-1} W_{k,m}(x) W_{\lambda,n}(x) &= \frac{\Gamma(2n) \Gamma(-m-n+\rho+1) \Gamma(m-n+\rho+1)}{\Gamma(n-\lambda+\frac{1}{2}) \Gamma(-k-n+\rho+\frac{3}{2})} \\
& {}_3F_2 \left(-n-\lambda+\frac{1}{2}, -m-n+\rho+1, m-n+\rho+1; 1-2n, -k-n+\rho+\frac{3}{2}; 1 \right) \\
& + \frac{\Gamma(-2n) \Gamma(-m+n+\rho+1) \Gamma(m+n+\rho+1)}{\Gamma(-n-\lambda+\frac{1}{2}) \Gamma(-k+n+\rho+\frac{3}{2})} \\
& {}_3F_2 \left(n-\lambda+\frac{1}{2}, -m+n+\rho+1, m+n+\rho+1; 2n+1, -k+n+\rho+\frac{3}{2}; 1 \right).
\end{aligned} \tag{5.16}$$

In order to evaluate the late time behaviour of complexity, the scheme is as follows. First we need to make the analytic continuation $u = \frac{\beta}{2} + it$ as before. Then plugging the resulting expression in the replica formula and taking the $N \rightarrow 0$, limit one can find the quantum expectation value of the geodesic length or equivalently, the complexity. Now since we are only interested in late time behaviour, the main contribution comes from the coincident limit, namely, $E_1 \rightarrow E_2$. It is convenient to use E and ω variables as defined in (5.7). Using (5.16) for our case, we get a nice expansion of the function $\mathcal{M}(N, E_1, E_2)$ in the limit $\omega \rightarrow 0$

$$\lim_{N \rightarrow 0} \frac{d}{dN} \mathcal{M}(N, E_1, E_2) = \frac{\sqrt{2E}}{2\pi\gamma_\mu(E)\hat{\rho}_D(E)} \frac{1}{\omega^2} + \text{local terms}. \tag{5.17}$$

However, in order to obtain the late time behaviour of complexity, we still need to perform the integrations over E and ω . Using this and the replica trick detailed above, one arrives at¹³

$$\begin{aligned}
\langle L(t) \rangle &= \text{const.} - \frac{e^{S_0}}{\pi Z_\mu(\beta)} \int_0^\infty dE e^{-\beta E} \sqrt{2E} \gamma_\mu(E) \hat{\rho}_D(E) \\
& \times \int_{-\infty}^\infty d\omega \frac{e^{i\omega t}}{\omega^2} \left(1 - \frac{\sin^2(\pi \hat{\rho}_D(E) e^{S_0} \omega)}{(\pi \hat{\rho}_D(E) e^{S_0} \omega)^2} \right).
\end{aligned} \tag{5.18}$$

It is worth stressing here that in order to derive the expression given in (5.18), one needs to take into account the non-perturbative effects explicitly through the sine-kernel appearing in the spectral correlation given in (3.6) [20].

It is now clear that the ω -integral may be performed exactly. In particular the expression in brackets on the right hand side of (5.18) corresponds to the disk contribution that results in linear growth. As was observed in [27], the disk linear growth is cancelled by the non-perturbative term as long as $2\pi\hat{\rho}_D(E)e^{S_0} \ll t$. It is easy to check that in this regime the integral vanishes identically.

On the other hand for $2\pi\hat{\rho}_D(E)e^{S_0} \gg t$, expanding the ‘‘sin’’-contribution in terms of

¹³Since we are interested in the time dependence of complexity, in this expression we have dropped a local term leading to a time independent term in the complexity and added all terms into the constant term. The corresponding term is divergent and has the form of $\delta(\omega)/\omega$.

exponentials and deforming the pole one finds [27]

$$\int_{-\infty}^{\infty} d\omega \frac{e^{i\omega t}}{\omega^2} \left(1 - \frac{\sin^2(\pi \hat{\rho}_D(E) e^{S_0} \omega)}{(\pi \hat{\rho}_D(E) e^{S_0} \omega)^2} \right) = \frac{2\pi^2 \hat{\rho}_D(E) e^{S_0}}{3} \left(1 - \frac{t}{2\pi \hat{\rho}_D(E) e^{S_0}} \right)^3. \quad (5.19)$$

Therefore overall

$$\langle L(t) \rangle = \text{const.} - \frac{2\pi e^{2S_0}}{3Z_\mu(\beta)} \int_{E_0}^{\infty} dE e^{-\beta E} \sqrt{2E} \gamma_\mu(E) \hat{\rho}_D^2(E) \left(1 - \frac{t}{2\pi \hat{\rho}_D(E) e^{S_0}} \right)^3. \quad (5.20)$$

Here E_0 is implicitly obtained via the equation $\pi \hat{\rho}_D(E_0) e^{S_0} = t$. Finally we have to perform the integral over E . To proceed, it is instructive to consider particular values of μ for which the above expression is simplified further. In what follows we will consider the case of $\mu = \frac{1}{2}$ as an illustrative example. In this case using the fact that

$$\gamma_{\frac{1}{2}}(E) = \frac{\pi \sqrt{2E}}{\sinh(\pi \sqrt{2E})}, \quad (5.21)$$

one gets

$$\langle L(t) \rangle = \text{const.} - \frac{4\pi^2 e^{2S_0}}{3Z_{\frac{1}{2}}(\beta)} \int_{E_0}^{\infty} dE e^{-\beta E} \frac{E \hat{\rho}_D^2(E)}{\sinh(\pi \sqrt{2E})} \left(1 - \frac{t}{2\pi \hat{\rho}_D(E) e^{S_0}} \right)^3, \quad (5.22)$$

where

$$Z_{\frac{1}{2}}(\beta) = e^{S_0} \int_0^{\infty} dE e^{-\beta E} \gamma_{\frac{1}{2}}(E) \hat{\rho}_D(E) = \frac{e^{\pi^2/2\beta} e^{S_0}}{\sqrt{2\pi} \beta^{3/2}} \left(1 + \frac{\pi^2}{\beta} \right). \quad (5.23)$$

For times $t \ll e^{S_0}$ one may expand the r.h.s of (5.22) and evaluate the integral which at leading order takes the form

$$\langle L(t) \rangle \approx \text{const.} - C_0 e^{S_0} + C_1 t, \quad (5.24)$$

where

$$C_0 = \frac{\pi^2 + 3\beta + 9e^{\frac{4\pi^2}{\beta}} (\beta + 3\pi^2)}{6\beta (\beta + \pi^2)},$$

$$C_1 = \frac{\sqrt{2} e^{-\frac{\pi^2}{2\beta}} \sqrt{\beta} (2\beta + \pi^2) + \pi^{3/2} (3\beta + \pi^2) \operatorname{erf}\left(\frac{\pi}{\sqrt{2}\sqrt{\beta}}\right)}{\sqrt{\pi} \beta (\beta + \pi^2)}. \quad (5.25)$$

For large t ($t \sim e^S$) the lower limit of the integral becomes large as well; $E_0 \rightarrow \infty$. Taking into account that the integrand itself has a factor of $e^{-\beta E}$ results in the fact that the integral decays and therefore the quantum expectation value of the geodesic length becomes constant. This can be interpreted as the saturation of complexity. For large t , one can estimate the rate by which the integral decays. For large t the lower limit of integral reads $E_0 = \frac{1}{8\pi^2} \ln^2(2\pi e^{-S_0} t)$. In this limit, approximating the ‘‘sinh’’ by an exponential

function one arrives at

$$\langle L(t) \rangle \approx \text{const.} - \frac{2\beta^{3/2} e^{-\frac{\pi^2}{2\beta}}}{3\pi^2 (\beta + \pi^2)} e^{S_0} e^{-\frac{\beta}{8\pi^2} \ln^2(2\pi e^{-S_0} t)} (e^{-S_0} t)^{3/2} \ln^2(2\pi e^{-S_0} t). \quad (5.26)$$

To summarise, our computation shows that the complexity grows linearly at late times up to $t \sim e^{S_0}$ and then saturates to a constant value of order e^{S_0} . Although we have demonstrated this behaviour explicitly only for a particular value of μ , the qualitative late time behaviour of complexity is the same for any value of μ .

5.3 The variance of complexity

Although the results of section 5 and the results of [27] exhibit late time behaviour in line with general expectations for complexity, this can be probed further by calculating the variance σ . Based on the procedure of computing the complexity in terms of the boundary-to-boundary two-point function, the variance of complexity has been evaluated in [27] where it was observed that the fluctuations exhibit linear growth at late times that is in tension with general expectations. In particular, this becomes especially problematic as the “noise” grows to the same size as the “signal” at $t \sim e^{2S_0}$.

Here we would like to use our approach based on the replica trick to compute the variance. To proceed let us focus on the two-sided case first to draw a direct comparison. Its generalisation to the one-sided case is then evident.

The variance has the structure

$$\sigma_\ell^2 = \langle \ell^2(u) \rangle - \langle \ell(u) \rangle^2 = \langle \ell^2(u) \rangle_C, \quad (5.27)$$

where we denote the connected contribution by C. Now in line with the rest of this section, it is clear that the quantity we have to determine is

$$\langle \ell^2(u) \rangle_C = \frac{4}{Z(\beta)} \int_0^\infty db_1 b_1 db_2 b_2 X(b_1, b_2) \int_0^\infty \frac{dy}{y} \Phi_T(\beta - u, b_1, \ell) \Phi_T(u, b_2, \ell) \left(\ln \frac{y}{4} \right)^2. \quad (5.28)$$

In order to calculate this we have to apply a replica type formula. We utilise the simple relation

$$\ln^2 A = \lim_{N \rightarrow 0} \frac{d^2}{dN^2} A^N. \quad (5.29)$$

By which the equation (5.28) may be recast into the following form

$$\begin{aligned} \langle \ell^2(u) \rangle_C &= \frac{1}{Z(\beta)} \lim_{N \rightarrow 0} \frac{d^2}{dN^2} \int_0^\infty b_1 db_2 b_2 db_2 X(b_1, b_2) \\ &\quad \times \int_0^\infty \frac{dy}{y} \Phi_T(\beta - u, b_1, \ell) \Phi_T(u, b_2, \ell) \left(\frac{y}{4} \right)^{2N}. \end{aligned} \quad (5.30)$$

This of course has a structure similar to the calculations of sections 5.1 and 5.2 and it is therefore clear that by making use of the trumpet wavefunction (2.29) one arrives at

$$\langle \ell^2(u) \rangle_C = \frac{4e^{-S_0}}{Z(\beta)} \int_0^\infty dE_1 dE_2 e^{-E_1(\beta-u) - E_2 u} \langle \rho(E_1) \rho(E_2) \rangle \left(\lim_{N \rightarrow 0} \frac{d^2}{dN^2} \mathcal{N}(N, E_1, E_2) \right), \quad (5.31)$$

which we analytically continue to

$$\langle \ell^2(t) \rangle_C = \frac{4e^{-S_0}}{Z(\beta)} \int_0^\infty dE \int_{-\infty}^\infty d\omega e^{-\beta E + i\omega t} \langle \rho(E + \frac{\omega}{2}) \rho(E - \frac{\omega}{2}) \rangle \left(\lim_{N \rightarrow 0} \frac{d^2}{dN^2} \mathcal{N}(N, E, \omega) \right), \quad (5.32)$$

where we are using the coordinates (5.7). At late times, taking the limit $\omega \rightarrow 0$, we have

$$\lim_{N \rightarrow 0} \frac{d^2}{dN^2} \mathcal{N}(N, E, \omega) = \frac{\sqrt{E}}{8\pi \hat{\rho}_D(E)} \left(\psi(2i\sqrt{2E}) + \psi(-2i\sqrt{2E}) - \ln 4 \right) \frac{1}{\omega^2} + \mathcal{O}(\omega^0), \quad (5.33)$$

where we have introduced the Polygamma function $\psi(x)$. This may then be used together with (3.6) to arrive at the final result

$$\begin{aligned} \langle \ell^2(t) \rangle_C &= \frac{e^{S_0}}{2\pi Z_D(\beta)} \int_0^\infty dE e^{-\beta E} \left(\psi(2i\sqrt{2E}) + \psi(-2i\sqrt{2E}) - \ln 4 \right) \hat{\rho}_D(E) \sqrt{E} \\ &\quad \times \int_{-\infty}^\infty d\omega \frac{e^{i\omega t}}{\omega^2} \left(1 - \frac{\sin^2(\pi \hat{\rho}_D(E) e^{S_0} \omega)}{(\pi \hat{\rho}_D(E) e^{S_0} \omega)^2} \right). \end{aligned} \quad (5.34)$$

We can see that the ω integration is of the same form as the one which appears in the calculation of the complexity itself.¹⁴ Indeed the only difference is the additional Polygamma structure. This is a pleasing result. The expression (5.34) circumvents the problematic late time growth of noise observed in [27]. The result saturates to a constant value and we therefore recover time-independent fluctuations before the recurrence time. We also observe that (5.34) implies a signal-to-noise ratio of order $\sim e^{-\frac{S_0}{2}}$ at $t \sim e^{S_0}$.

For the one-sided black hole the procedure is the same and indeed we recover a similar expression with a rather more complicated E -dependent function that comes from the fact that

$$\lim_{N \rightarrow 0} \frac{d^2}{dN^2} \mathcal{M}(N, E, \omega) = \frac{1}{\hat{\rho}_D(E)} \frac{F(E, \mu)}{\omega^2} + \mathcal{O}(\omega^0), \quad (5.35)$$

where we introduced $F(E, \mu)$, which is a complicated function of E and μ containing hypergeometric and polygamma functions and their derivatives.

6 Conclusion and Outlook

In this work, we have considered a fixed EOW brane which plays the role of a cutoff by removing a part of boundary. This setup provides a holographic model for a one-sided black hole. We have computed the multi-boundary partition functions and the matter correlation functions in this model. However, the most important result in this work is the computation of complexity.

To compute complexity we have employed a modified version of the well-known replica trick used to study the quenched free energy. This avoids the ambiguity of defining complexity in terms of boundary-to-boundary correlation functions as advocated for in [27]. The

¹⁴Note that in this expression we have not considered a contact term that is proportional to a delta function. As we mentioned in the calculation of complexity, this term being of the form of $\delta(\omega)/\omega$ leads to a time independent term which does not contribute to complexity growth. In the present case this term gives a divergent term which could be removed by subtracting $\ell(0)$. Although it is important to consider this term in the computation of variance, since our aim was to show how the replica trick results in a reasonable variance, we have just considered $\ell^2(t)$ and dropped the corresponding term by hand.

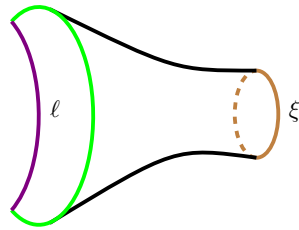


Figure 6: Trumpet capped by the FZZT brane shown by a brown circle and parametrized by ξ .

tension between the limit of scaling dimensions and the geodesic approximation is therefore not present in this work. We have retrieved the expected non-perturbative plateau regime in the late time growth of complexity, which follows an early period of perturbative linear growth in time. Although the result is qualitatively similar to that of a two-sided black hole, except for the coefficients being sensitive to the tension of the EOW brane now, the replica trick employed in our work yields a more satisfactory result for the variance. The emergence of only time-independent fluctuations in the variance compared to the late-time linear growth of [27] would seem an advancement in the calculation of the black hole volume in JT gravity. Of course in our approach the geometric picture is less obvious.

We will now conclude with a couple of interesting and related questions which are in progress.

Dynamical EOW branes So far we have considered a fixed EOW brane without any associated dynamics. However, it is interesting to consider a dynamical EOW brane. This requires considering a certain EOW brane that contributes to the path integral. In other words, one could imagine a general hypersurface with some of geodesics capped by EOW branes.

To start with we can start with a toy model where the geodesic of a trumpet geometry is capped off by an Fateev-Zamolodchikov-Zamolodchikov-Teschner (FZZT) anti-brane [61, 62] as shown in fig. 6. Following the prescription of [63], what we need to do is insert a factor of $-\frac{1}{b}e^{-\xi b}$ in the path integral on a trumpet with parameter b .

In order to see the effect of this brane on the behaviour of complexity as a function of time, following the procedure we adopted for the EOW brane, one first needs to construct the corresponding wavefunction in presence of the FZZT anti-brane. In what follows, for simplicity, we shall consider two-sided black holes. Starting from $\Phi_T(\beta, b, \ell)$ given in (2.29), one can compute the wavefunction associated with fig. 6 as

$$\Phi_T(\beta, \ell) = - \int_0^\infty db e^{-\xi b} \Phi_T(\beta, b, \ell) = - \frac{4e^{-S_0/2}}{\pi} \int_0^\infty dk e^{-\frac{\beta k^2}{2}} \frac{\xi}{\xi^2 + k^2} K_{2ik}(y). \quad (6.1)$$

With this result in hand, we need to employ our modified replica method defined

through (5.3) which yields, at late time,

$$\langle \ell(t) \rangle = \text{Const.} + \frac{1}{\pi^3 \tilde{Z}(\beta)} \int_0^\infty \frac{dE}{2E} e^{-\beta E} \left[\pi \xi \kappa \frac{2\sqrt{2E} \hat{\rho}_D(E)}{\xi^2 + 2E} - \frac{\kappa^2 \xi^2 e^{-S_0}}{(\xi^2 + 2E)^2} \right] \times \frac{\sqrt{2E}}{\hat{\rho}_D(E)} \int_{-\infty}^\infty d\omega \frac{e^{i\omega t}}{\omega^2}, \quad (6.2)$$

where κ is the number of FZZT anti-branes. Since we are only interested in the late time behaviour, we have used the E and ω variables (5.7) in the coincident limit, $E_1 \rightarrow E_2$.

The ω -integral of (6.2) can be readily performed and yields

$$\langle \ell(t) \rangle = \text{Const.} - \frac{t}{\pi^2 \tilde{Z}(\beta)} \int_0^\infty \frac{dE}{2E} e^{-\beta E} \left[\pi \xi \kappa \frac{2\sqrt{2E} \hat{\rho}_D(E)}{\xi^2 + 2E} - \frac{\kappa^2 \xi^2 e^{-S_0}}{(\xi^2 + 2E)^2} \right] \frac{\sqrt{E}}{\hat{\rho}_D(E)}. \quad (6.3)$$

From (6.3) it is clear that whether the above contribution results in a decreasing or increasing behaviour of complexity at late times depends on the E integral. Note that the disk contribution is proportional to e^{S_0} whereas the above contribution is given in terms of the number of branes κ , therefore one might naively expect an interesting competition between κ and e^{S_0} that is similar to that of entanglement entropy. We hope to report the final conclusion, both for the two-sided and one-sided black hole geometries, soon [64]. We expect this computation to shed light on the physical interpretation of the replica procedure we employed to compute complexity.

UV cutoff In this paper we discussed EOW branes playing the role of cutoffs. In the Lorentzian version of the theory, the cutoff EOW brane lies behind the event horizon of the black hole. In holographic theories, there is an interesting correspondence between a UV cutoff near the boundary of AdS spacetime and a conformal field theory deformed by a particular irrelevant operator quadratic in the stress-energy tensor [65–67], namely, the $T\bar{T}$ deformation [68–70]. The wavefunction technique we used for the EOW brane will also be useful in computing complexity for a $T\bar{T}$ -deformed CFT.

The partition function of $T\bar{T}$ deformed JT gravity may be written as [71]

$$Z_{D,\lambda}(\beta) = \int_{-\infty}^\infty dE e^{-\beta f(E)} \hat{\rho}_D(E), \quad (6.4)$$

where $f(E) = \frac{1 - \sqrt{1 - 8\lambda E}}{4\lambda}$, λ is the deformation parameter and E , the energy of the undeformed theory. Clearly for $\lambda \rightarrow 0$ one finds the standard partition function.

Our aim is to compute the complexity for this deformed version of JT gravity. As mentioned above, we will use the wavefunction formalism. To do so, one needs to write down the corresponding disk wave function for the deformed theory. Using the formalism developed in [71] for $\lambda < 0$ one can easily find the deformed wavefunction as

$$\Phi_{D,\lambda}(\beta, \ell) = 4e^{S_0/2} \int_0^\infty dE e^{-\beta f(E)} \hat{\rho}_D(E) K_{2i\sqrt{2E}}(y). \quad (6.5)$$

which exactly reproduces the partition function (6.4).

Once we have the wavefunction (6.5), we can once again use the modified replica method (5.3) to compute complexity. In the late time limit, using the coincident variables

(5.7), we obtain

$$\langle \ell(t) \rangle \sim \text{const.} - \frac{2e^{S_0}}{\sqrt{2\pi Z_\lambda(\beta)}} \int_0^\infty dE e^{-\beta f(E)} \sqrt{E} \hat{\rho}_D(E) \int_{-\infty}^\infty d\omega \frac{e^{\frac{i\omega}{\sqrt{1-8\lambda E}}}}{\omega^2}. \quad (6.6)$$

The integral over ω can be performed exactly and we arrive at the following expression at late time showing linear growth of complexity, as expected from the disk level computation.

$$\langle \ell(t) \rangle \sim \text{const.} + \frac{2e^{S_0 t}}{\sqrt{2} Z_\lambda(\beta)} \int_0^\infty dE e^{-\beta f(E)} \frac{\sqrt{E} \hat{\rho}_D(E)}{\sqrt{1-8\lambda E}}. \quad (6.7)$$

While obtaining the plateau regime of complexity in this setup can be done straightforwardly by adding higher genus contributions as before, it will be interesting to study the saturation of complexity in this deformed JT setup in presence of an EOW brane. We postpone this for future work.

Acknowledgments

We would like to thank Moritz Dorband, Johanna Erdmenger and Misha Usatyuk for helpful discussions.

References

- [1] J.M. Maldacena, *The Large N limit of superconformal field theories and supergravity*, *Adv. Theor. Math. Phys.* **2** (1998) 231 [[hep-th/9711200](#)].
- [2] E. Witten, *Anti-de Sitter space and holography*, *Adv. Theor. Math. Phys.* **2** (1998) 253 [[hep-th/9802150](#)].
- [3] S.S. Gubser, I.R. Klebanov and A.M. Polyakov, *Gauge theory correlators from noncritical string theory*, *Phys. Lett. B* **428** (1998) 105 [[hep-th/9802109](#)].
- [4] L. Susskind, *Computational Complexity and Black Hole Horizons*, *Fortsch. Phys.* **64** (2016) 24 [[1403.5695](#)].
- [5] L. Susskind, *Three Lectures on Complexity and Black Holes*, SpringerBriefs in Physics, Springer, 10, 2018, DOI [[1810.11563](#)].
- [6] D. Stanford and L. Susskind, *Complexity and Shock Wave Geometries*, *Phys. Rev. D* **90** (2014) 126007 [[1406.2678](#)].
- [7] A.R. Brown, D.A. Roberts, L. Susskind, B. Swingle and Y. Zhao, *Holographic Complexity Equals Bulk Action?*, *Phys. Rev. Lett.* **116** (2016) 191301 [[1509.07876](#)].
- [8] A.R. Brown, D.A. Roberts, L. Susskind, B. Swingle and Y. Zhao, *Complexity, action, and black holes*, *Phys. Rev. D* **93** (2016) 086006 [[1512.04993](#)].
- [9] L. Susskind, *The Typical-State Paradox: Diagnosing Horizons with Complexity*, *Fortsch. Phys.* **64** (2016) 84 [[1507.02287](#)].
- [10] A.R. Brown, L. Susskind and Y. Zhao, *Quantum Complexity and Negative Curvature*, *Phys. Rev. D* **95** (2017) 045010 [[1608.02612](#)].
- [11] V. Balasubramanian, M. Decross, A. Kar and O. Parrikar, *Quantum Complexity of Time Evolution with Chaotic Hamiltonians*, *JHEP* **01** (2020) 134 [[1905.05765](#)].
- [12] L. Susskind, *Black Holes at Exp-time*, [2006.01280](#).

- [13] V. Balasubramanian, M. DeCross, A. Kar, Y.C. Li and O. Parrikar, *Complexity growth in integrable and chaotic models*, *JHEP* **07** (2021) 011 [2101.02209].
- [14] J. Haferkamp, P. Faist, N.B.T. Kothakonda, J. Eisert and N.Y. Halpern, *Linear growth of quantum circuit complexity*, 2106.05305.
- [15] C. Teitelboim, *Gravitation and Hamiltonian Structure in Two Space-Time Dimensions*, *Phys. Lett. B* **126** (1983) 41.
- [16] R. Jackiw, *Lower Dimensional Gravity*, *Nucl. Phys. B* **252** (1985) 343.
- [17] J. Maldacena, D. Stanford and Z. Yang, *Conformal symmetry and its breaking in two dimensional Nearly Anti-de-Sitter space*, *PTEP* **2016** (2016) 12C104 [1606.01857].
- [18] J. Engelsöy, T.G. Mertens and H. Verlinde, *An investigation of AdS_2 backreaction and holography*, *JHEP* **07** (2016) 139 [1606.03438].
- [19] P. Saad, S.H. Shenker and D. Stanford, *A semiclassical ramp in SYK and in gravity*, 1806.06840.
- [20] P. Saad, S.H. Shenker and D. Stanford, *JT gravity as a matrix integral*, 1903.11115.
- [21] P. Saad, *Late Time Correlation Functions, Baby Universes, and ETH in JT Gravity*, 1910.10311.
- [22] A. Altland and J. Sonner, *Late time physics of holographic quantum chaos*, *SciPost Phys.* **11** (2021) 034 [2008.02271].
- [23] A. Belin and J. de Boer, *Random statistics of OPE coefficients and Euclidean wormholes*, *Class. Quant. Grav.* **38** (2021) 164001 [2006.05499].
- [24] J. Cotler and K. Jensen, *AdS_3 gravity and random CFT*, *JHEP* **04** (2021) 033 [2006.08648].
- [25] A. Almheiri, T. Hartman, J. Maldacena, E. Shaghoulian and A. Tajdini, *Replica Wormholes and the Entropy of Hawking Radiation*, *JHEP* **05** (2020) 013 [1911.12333].
- [26] G. Penington, S.H. Shenker, D. Stanford and Z. Yang, *Replica wormholes and the black hole interior*, 1911.11977.
- [27] L.V. Iliesiu, M. Mezei and G. Sárosi, *The volume of the black hole interior at late times*, 2107.06286.
- [28] M. Mirzakhani, *Simple geodesics and Weil-Petersson volumes of moduli spaces of bordered Riemann surfaces*, *Invent. Math.* **167** (2006) 179.
- [29] J.M. Deutsch, *Quantum statistical mechanics in a closed system*, *Phys. Rev. A* **43** (1991) 2046.
- [30] M. Srednicki, *Chaos and quantum thermalization*, *Phys. Rev. E* **50** (1994) 888.
- [31] K. Okuyama and K. Sakai, *Multi-boundary correlators in JT gravity*, *JHEP* **08** (2020) 126 [2004.07555].
- [32] I. Kourkoulou and J. Maldacena, *Pure states in the SYK model and nearly- AdS_2 gravity*, 1707.02325.
- [33] J.M. Maldacena, *Eternal black holes in anti-de Sitter*, *JHEP* **04** (2003) 021 [hep-th/0106112].
- [34] P. Gao, D.L. Jafferis and D.K. Kolchmeyer, *An effective matrix model for dynamical end of the world branes in Jackiw-Teitelboim gravity*, *JHEP* **01** (2022) 038 [2104.01184].
- [35] D. Harlow and D. Jafferis, *The Factorization Problem in Jackiw-Teitelboim Gravity*, *JHEP* **02** (2020) 177 [1804.01081].
- [36] C.V. Johnson, *Nonperturbative Jackiw-Teitelboim gravity*, *Phys. Rev. D* **101** (2020) 106023 [1912.03637].

- [37] C.V. Johnson, *Explorations of nonperturbative Jackiw-Teitelboim gravity and supergravity*, *Phys. Rev. D* **103** (2021) 046013 [[2006.10959](#)].
- [38] C.V. Johnson, *The Microstate Physics of JT Gravity and Supergravity*, [2201.11942](#).
- [39] Z. Yang, *The Quantum Gravity Dynamics of Near Extremal Black Holes*, *JHEP* **05** (2019) 205 [[1809.08647](#)].
- [40] L. Susskind and Y. Zhao, *Switchbacks and the Bridge to Nowhere*, [1408.2823](#).
- [41] K. Jensen, *Chaos in AdS₂ Holography*, *Phys. Rev. Lett.* **117** (2016) 111601 [[1605.06098](#)].
- [42] R. Szmytkowski and S. Bielski, *An orthogonality relation for the whittaker functions of the second kind of imaginary order*, [0910.1492](#).
- [43] B. Eynard and N. Orantin, *Weil-Petersson volume of moduli spaces, Mirzakhani's recursion and matrix models*, [0705.3600](#).
- [44] D. Stanford and E. Witten, *Fermionic Localization of the Schwarzian Theory*, *JHEP* **10** (2017) 008 [[1703.04612](#)].
- [45] A. Blommaert, *Dissecting the ensemble in JT gravity*, [2006.13971](#).
- [46] J.S. Cotler, G. Gur-Ari, M. Hanada, J. Polchinski, P. Saad, S.H. Shenker et al., *Black Holes and Random Matrices*, *JHEP* **05** (2017) 118 [[1611.04650](#)].
- [47] D. Bagrets, A. Altland and A. Kamenev, *Power-law out of time order correlation functions in the SYK model*, *Nucl. Phys. B* **921** (2017) 727 [[1702.08902](#)].
- [48] T.G. Mertens, G.J. Turiaci and H.L. Verlinde, *Solving the Schwarzian via the Conformal Bootstrap*, *JHEP* **08** (2017) 136 [[1705.08408](#)].
- [49] A. Kitaev and S.J. Suh, *Statistical mechanics of a two-dimensional black hole*, *JHEP* **05** (2019) 198 [[1808.07032](#)].
- [50] M. Srednicki, *The approach to thermal equilibrium in quantized chaotic systems*, *Journal of Physics A: Mathematical and General* **32** (1999) 1163–1175.
- [51] M. Miyaji, T. Takayanagi and T. Ugajin, *Spectrum of End of the World Branes in Holographic BCFTs*, *JHEP* **06** (2021) 023 [[2103.06893](#)].
- [52] B. Eynard, *Topological expansion for the 1-Hermitian matrix model correlation functions*, *JHEP* **11** (2004) 031 [[hep-th/0407261](#)].
- [53] B. Eynard and N. Orantin, *Invariants of algebraic curves and topological expansion*, *Commun. Num. Theor. Phys.* **1** (2007) 347 [[math-ph/0702045](#)].
- [54] F. Wegner, *The mobility edge problem: Continuous symmetry and a conjecture*, *Zeitschrift für Physik B Condensed Matter* **35** (1979) 207.
- [55] K.B. Efetov, *Supersymmetry and theory of disordered metals*, *Adv. Phys.* **32** (1983) 53.
- [56] N. Engelhardt, S. Fischetti and A. Maloney, *Free energy from replica wormholes*, *Phys. Rev. D* **103** (2021) 046021 [[2007.07444](#)].
- [57] C.V. Johnson, *Low Energy Thermodynamics of JT Gravity and Supergravity*, [2008.13120](#).
- [58] C.V. Johnson, *On the Quenched Free Energy of JT Gravity and Supergravity*, [2104.02733](#).
- [59] M. Alishahiha, A. Faraji Astaneh, G. Jafari, A. Naseh and B. Taghavi, *Free energy for deformed Jackiw-Teitelboim gravity*, *Phys. Rev. D* **103** (2021) 046005 [[2010.02016](#)].
- [60] I.S. Gradshteyn, I.M. Ryzhik, D. Zwillinger and V. Moll, *Table of integrals, series, and products; 8th ed.*, Academic Press, Amsterdam (Sep, 2014), [0123849330](#).
- [61] V. Fateev, A.B. Zamolodchikov and A.B. Zamolodchikov, *Boundary Liouville field theory. 1. Boundary state and boundary two point function*, [hep-th/0001012](#).

- [62] J. Teschner, *Remarks on Liouville theory with boundary*, *PoS tnr2000* (2000) 041 [[hep-th/0009138](#)].
- [63] K. Okuyama and K. Sakai, *FZZT branes in JT gravity and topological gravity*, *JHEP* **09** (2021) 191 [[2108.03876](#)].
- [64] M. Alishahiha, S. Banerjee and J. Kames-King, *To appear soon*, .
- [65] L. McGough, M. Mezei and H. Verlinde, *Moving the CFT into the bulk with $T\bar{T}$* , *JHEP* **04** (2018) 010 [[1611.03470](#)].
- [66] M. Taylor, *TT deformations in general dimensions*, [1805.10287](#).
- [67] T. Hartman, J. Kruthoff, E. Shaghoulian and A. Tajdini, *Holography at finite cutoff with a T^2 deformation*, *JHEP* **03** (2019) 004 [[1807.11401](#)].
- [68] A.B. Zamolodchikov, *Expectation value of composite field T anti- T in two-dimensional quantum field theory*, [hep-th/0401146](#).
- [69] F.A. Smirnov and A.B. Zamolodchikov, *On space of integrable quantum field theories*, *Nucl. Phys. B* **915** (2017) 363 [[1608.05499](#)].
- [70] A. Cavaglià, S. Negro, I.M. Szécsényi and R. Tateo, *$T\bar{T}$ -deformed 2D Quantum Field Theories*, *JHEP* **10** (2016) 112 [[1608.05534](#)].
- [71] L.V. Iliesiu, J. Kruthoff, G.J. Turiaci and H. Verlinde, *JT gravity at finite cutoff*, *SciPost Phys.* **9** (2020) 023 [[2004.07242](#)].